CHEMICAL ENGINEERING TRANSACTIONS
VOL. 108, 2024
A publication of AIDIC
The Italian Association of Chemical Engineering
Online at www.cetjournal.it
Guest Editors: Carlo Pirola, Antonio Espuña

ISBN 979-12-81206-08-3; **ISSN** 2283-9216
DOI: 10.3303/CET24108002

Monitoring Adsorption kinetics with Surface-enhanced Raman Scattering in a Microfluidic Environment

Victoria Fournier, Aristides Docoslis*

Department of Chemical Engineering, Queen's University, Kingston, ON K7L 3N6 Canada
docoslis@queensu.ca

This article provides a proof of concept on how Surface-enhanced Raman Scattering (SERS) can be combined with microfluidics towards the development of an in situ chemical detection method. A microfluidic device prototype was designed, fabricated, and characterized to demonstrate the feasibility of microfluidics in achieving analyte transport from the sample introduction site to the detection site. Subsequently, the microfluidic setup was used for monitoring the adsorption kinetics of the molecule rhodamine 6G (R6G) onto a SERS-active substrate; an application, for which only scare information is available in the literature. Moreover, this work demonstrates how the actual concentration of adsorbed R6G (moles m^{-2}) onto the SERS substrate can be quantified in real time. SERS-active substrates, such the ones used in this study, can be integrated in a microfluidic device for achieving reproducible monitoring of the adsorption kinetics of a molecule in a liquid sample, or for detecting and reporting the concentration of an unknown target molecule during a diagnostic assay.

1. Introduction

The increasing need for point-of-care (POC) diagnostic devices creates a strong incentive to integrate established laboratory chemical detection and quantification methods with microfluidic, lab-on-a-chip (LOC), systems (Maria et al., 2017; Juncker et al., 2002). The incorporation of microfluidics into chemical analysis allow for greater control of the introduction of analyte to the detection method of choice. Surface-enhanced Raman Scattering (SERS) is an advantageous detection method due to its non-destructive, rapid, chemically specific and ultrasensitive detection characteristics. Applications of a variety of SERS detection methods in LOC devices have been reported in literature (White et al., 2013; Kong et al., 2018; Andreou et al., 2013). These applications show success at overcoming various limitations of the SERS detection method by demonstrating ease of use, speed of measurement, accuracy and reproducibility of results. However, current SERS detection methods incorporated into LOC devices all share a similar disadvantage: Samples must be mixed with nanoparticles before being loaded into the device. This sample preparation step increases the difficulty of use of the device in a POC diagnostic setting and presents the issue of nanoparticles crashing out of solution before sample loading. Recently, a patented technique that creates SERS-active substrates with the use of electric field-directed nanoparticle assembly has been developed in our lab (Bacon at al., 2022; Dies et al., 2017). The produced SERS substrates have been shown to amplify the conventional Raman signal by more than 10^6-fold. The substrates have been successful in the detection and quantification of a variety of samples, including illicit drugs [Wilson et al., 2021], environmental pollutants [Raveendran et al., 2021], and food adulterants (Dies et al., 2018). However, all the tests were performed by following the standard method of "drop-casting", *i.e.*, placing a droplet of the liquid sample on the surface of the sensor and waiting for the liquid in the droplet to evaporate. A major disadvantage of drop-casting is that it results in an uneven target molecule distribution on the surface, consequentially impeding the reproducibility and reliability of the detection method. The cause of uneven distribution can be attributed to droplet evaporation that results in the "coffee-ring" effect that concentrates analyte deposition towards the outer circumference of the drop (Shur et al., 2015). Another limitation to the drop-cast method is the amount of time needed for evaporation to occur. The slow rate of introduction of target

Paper Received: 19 August 2023 ; Revised: 10 November 2023 ; Accepted: 19 January 2024
Please cite this article as: Fournier V., Docoslis A., 2024, Monitoring Adsorption Kinetics with Surface-enhanced Raman Scattering in a Microfluidic Environment, Chemical Engineering Transactions, 108, 7-12 DOI:10.3303/CET24108002

molecule to SERS substrate impedes the use of the technique in POC diagnostics, since measurements need to be taken instantaneously.

Before these new SERS substrates can be implemented into POC diagnostics, new sample introduction methods must be investigated such that target molecules are arranged evenly on the substrates, resulting in greater reproducibility and reliability. A uniform and gradual sample introduction into the SERS-active surface may also help overcome limitations with the ability of SERS to provide quantifiable results. Therefore, the combination of these new SERS substrates with microfluidics appears to hold promise for overcoming some of the main disadvantages that presently exist with the application of the method in the field.

This article is a demonstration of how SERS-active substrates can be combined with microfluidics toward the development of an in situ chemical detection method that can be used as a POC diagnostic device. A microfluidic device prototype was designed, fabricated, and characterized to demonstrate the feasibility of microfluidics in achieving analyte transport from loading to detection site. More importantly, this basic microfluidic setup is used here for monitoring the adsorption kinetics of the molecule rhodamine 6G (R6G) onto a SERS-active substrate; an application, for which only scare information is available in the literature. In fact, we take this application a step further by showing how to quantify in real time the actual concentration of adsorbed R6G onto the SERS substrate. We offer a proof of concept on how we can use a SERS-active substrate embedded in a diagnostic microfluidic device to detect and report the concentration of an unknown target molecule in an aqueous solution as a function of time.

2. Experimental Details

Materials.

Polydimethylsiloxane (PDMS), Sylgard™ elastomer kit with monomer and curing agent, was purchased from Dow Corning Corporation (Midland, MI, USA). Polylactic acid (PLA) 3D Printer Filament was purchased from AMZ3D. Diiodomethane (99%) and rhodamine 6G (R6G, 99%) were purchased from Sigma-Aldrich (Oakville, ON). Silver nanoparticles (AgNPs), 50nm in diameter, were bought from Cytodiagnostics Inc. (Burlington, ON). Polished silicon wafers (4” diameter) with a thermally grown SiO_2 layer (0.5 µm) were purchased from University Wafer (South Boston, MA, USA). Millipore® water (18.2 MΩ cm) was used in all experiments to prepare R6G stock solutions.

Methods

Microfluidic device. A negative mold of the microfluidic prototype was designed and modelled using SolidWorks. The mold was printed using a 3D FDM (Fusion Deposition Modeling) printer (IIIP Mini 3D Printer), with PLA as the print material. Prototypes were cast in PDMS using a monomer base-to-curing agent ratio of 10:1. Each batch was mixed for 5 minutes and degassed in a vacuum at 0.7 MPa for 30 minutes before being poured into the mold. Microfluidic chips were allowed to cure on a hotplate at 80 ˚C for 2-3 hours. The PDMS chip was rendered hydrophilic through oxygen plasma treatment, using a Harrick Plasma Cleaner (Model: PDC32G) for 5 minutes. Microfluidic prototypes were assembled by contacting the PDMS chips with glass substrates and letting them bond on a hotplate at 80 ˚C for 20 minutes. Inlet and outlet reservoirs each have a radius of 3 mm for SERS substrate integration. The channel connecting the reservoirs has a length of 30 mm and a cross-sectional area of 1 mm by 1 mm.

Sample Preparation and Fluorescence Measurements. Six aliquots (1 mL) of AgNP dispersion were concentrated through centrifugation at 3600g for 30 minutes. The supernatant was discarded from each sample and the isolated AgNPs were placed into R6G solutions of five concentrations (5*10-8 M, 10-7 M, 5*10-7 M, 10-6 M and 5*10-6 M) and a control solution of water (5 mL each). Solutions of R6G were sonicated to ensure full dispersion of AgNPs and were left to adsorb for 24 hours. Solutions were centrifuged again at the same conditions, followed by removing the supernatant. The supernatant was retained and used for fluorescence spectroscopy measurements. Fluoresce spectral data was collected using a PTI QuantaMaster™ 80 Fluorometer with a Xenon arc lamp and dual PMT detectors. Data was collected using the emission scan method over a range of 500 nm to 650 nm with an excitation wavelength of 532 nm, step size of 0.5 nm, integration time of 1 second and a blank water sample as the background. A total of three spectra were collected for each sample tested to determine the experimental error.

SERS substrate fabrication. The procedure is described in detail in Dies et al., 2017. Briefly, the microchip electrodes were fabricated at the Nanofabrication Kingston facility (NFK, Innovation Park, Kingston, ON). The negative photoresist SU-8 (MicroChem Corp, Westborough, MA) and maskless photolithography were used to transfer the microelectrode pattern on to silicon wafers. Subsequent electron beam metal film evaporation and lift off completed the microchips. A layer of chrome (5 µm) was implemented on the silicon wafer to enhance the

adhesion of gold electrodes (100 µm thickness). Next, AgNPs were assembled by dispensing a 10 µL drop over the center of the microelectrodes. Each SERS substrate was allowed to accumulate on the microchip for 5 minutes at an AC frequency of 10 Hz and a peak-to-peak voltage of 3 V. Microchips were rinsed with water and dried under a stream of air before use in further experiments.

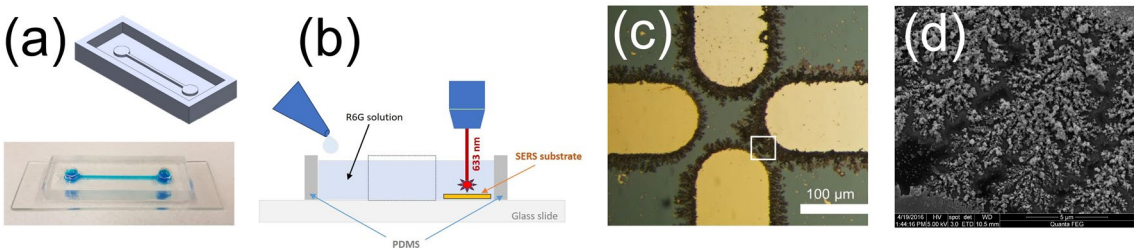

Figure 1: (a) Mold of microfluidic prototype. (b) Schematic depicting the cross sectional view of the assembled microfluidic device during a SERS measurement. (c) SERS-active dendritic AgNP structures formed in the interelectrode spaces. (d) SEM image showing details on the AgNP structure.

Adsorption Measurements. SERS substrates affixed at the bottom of the receiving reservoir of the microfluidic cell were placed under the Raman microscope. Solutions of known concentration of R6G were dispensed in the feeding reservoir and were let to flow over the SERS substrate in the receiving reservoir. Adsorption was monitored over time such that SERS measurements were taken through the air and aqueous solution above the chip. The SERS spectra were collected using a HORIBA-Jobin Yvon Raman Spectrometer (Model: LabRAM) with a 632.8 nm He/Ne laser (17 mW), 1800 l mm^{-1} grating and an Olympus BX-41 microscope system. The spectra were measured with 10x microscope objective for 3x5 s for each measurement. A background baseline correction and Savitsky-Golay filter was applied to all spectral data using MATLAB. Adsorption isotherm model fitting was also performed using an open-source MATLAB code11.

3. Results and Discussion

To be able to quantify the concentration of adsorbed R6G on the SERS substrate, an adsorption isotherm was first created that correlates the amount of R6G (moles m^{-2}) adsorbed on the AgNP to the concentration of R6G in solution (moles L^{-1}) at equilibrium. This correlation is subsequently used to link the SERS signal intensity to the concentration of adsorbed R6G, as described below. This is possible due to the unique advantage of the present SERS substrate fabrication technique, namely, the AgNPs used for constructing the adsorption isotherm also serve as building blocks of the dendritic SERS. Fig. 1c is a top-down microscope image of the dendritic substrates formed in the gaps between planar microelectrodes using our electric field-guided AgNP assembly technique, while Fig. 1d is an SEM image showing details of that SERS-active AgNP structure. The enhancement factor provided by these Ag dendritic substrates was found to be equal to $4x10^5$ (Dies et al., 2017). A step-by-step presentation of the method that allows quantification of adsorbed R6G is described below.

Construction of the R6G adsorption isotherm. First, a calibration curve for measuring the concentration of R6G in solution was constructed using fluorescence spectroscopy. A control (DI water) and five aqueous solutions of R6G ranging in concentration from $5*10^{-8}$ M to $5*10^{-6}$ M were used for the measurements (Fig. 2a). Background noise correction and linear regression analyses were performed on the data. Data point regression produced a linear correlation (R^2=0.999).

Next, 50nm AgNPs (concentration: $2x10^{10}$ nanoparticles/mL; corresponding surface area: 2.28 cm^2/mL) dispersed into the control and five aqueous solutions of R6G were used to generate the adsorption isotherm. In each case, the surface concentration (mole m^{-2}) of R6G adsorbed onto the AgNPs was calculated by concentration difference (initial vs. equilibrium) and knowledge of the total surface area provided by the AgNPs. Adsorption equilibrium was assumed to be reached within 24 hours. After allowing 24 hours for R6G molecules to adsorb onto AgNPs in the solution, AgNPs were centrifuged out of the solution. Fluorescence spectroscopy were obtained for the remaining supernatants of each solution. Unknown concentrations of supernatant solutions were determined by using the calibration curve for R6G (Fig. 2a). The concentration of each supernatant was assumed to be equivalent to the equilibrium bulk concentration at adsorption equilibrium. Figure 2b shows the R6G adsorption isotherm generated from experimental data. The R6G adsorption isotherm was fit with a linear model.

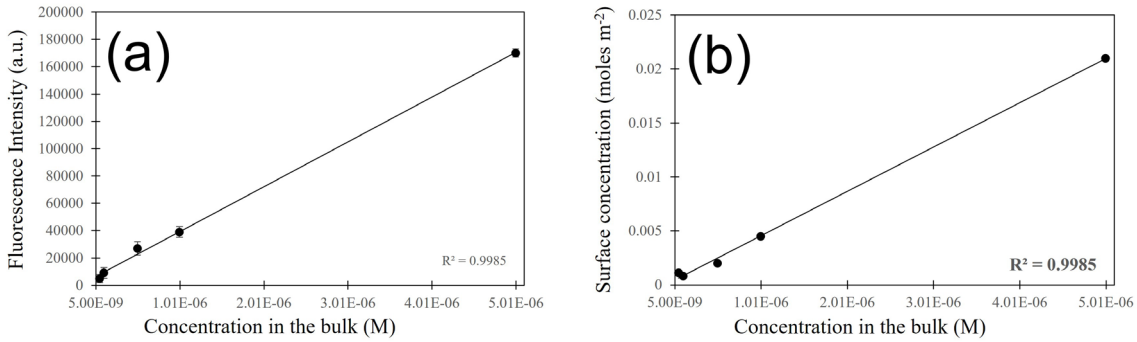

Figure 2: (a) Calibration curves for R6G in solution; (b) R6G isotherm

Correlating Raman Intensity and R6G Adsorption. The SERS intensity can be correlated to the concentration of analyte in solution. The Raman spectra for R6G has several distinct, strong peaks from which intensity can be monitored. Here, changes in the R6G spectrum intensity are monitored using the strong C-C in-plane bending peak at 612 cm^{-1}. A calibration curve following this characteristic peak intensity was constructed using SERS spectroscopy for five aqueous solutions of R6G ranging in concentration from $5*10^{-8}$ M to $5*10^{-6}$ M (Fig. 3a). A linear regression analysis was performed on the data and the calibration curve also demonstrated a strong linear dependence (R^2=0.9868).

Distribution of R6G on the SERS substrate through adsorption allows for correlation of Raman intensity with concentration of R6G on the SERS substrate. The experimental R6G adsorption isotherm onto AgNPs (Fig. 3b) predicts the concentration of R6G that will be adsorbed onto an AgNPs surface dependent on bulk equilibrium concentration. The SERS measurements were performed after equilibrium has been reached between R6G molecules and the AgNP substrate. Through this assumption, SERS signal intensities measured for known initial bulk R6G concentrations can be correlated to the adsorbed R6G concentrations for the same known initial bulk R6G concentrations. Figure 3b demonstrates the direct correlation of R6G adsorbed concentration versus Raman intensity. The regressed data in Figure 3b show a linear correlation (R^2=0.9911) and validates its use in determining the concentration of R6G adsorbed on the surface of SERS substrates from Raman intensity values.

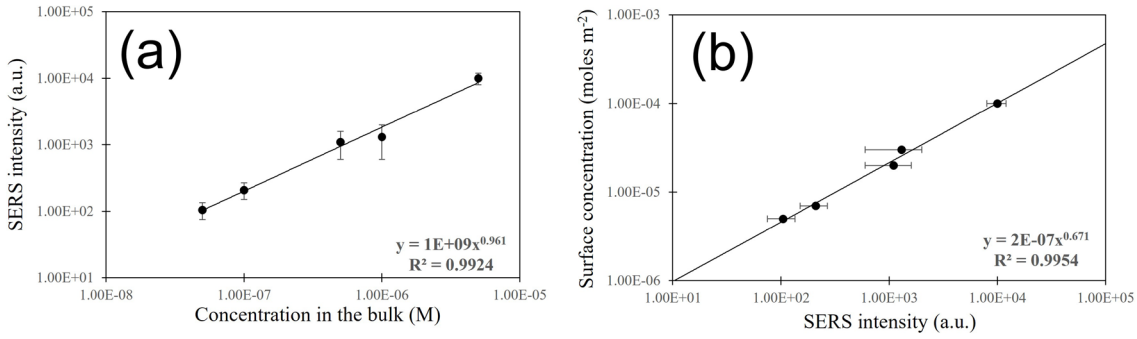

Figure 3: (a) R6G SERS intensity (612 cm^{-1} peak) vs. R6G in solution; (b) Correlation between SERS signal intensity (612 cm^{-1} peak) and adsorbed R6G.

Kinetics of R6G adsorption. Figure 4 shows an example of how the progression of R6G adsorption onto the SERS substrate can be monitored by recording the intensity of the SERS spectra. The complete set of results from this study are presented in Fig. 5. SERS substrates were exposed to aqueous solutions of R6G at initial bulk concentrations of $5*10^{-7}$ M, $1*10^{-6}$ M and $5*10^{-6}$ M. Adsorption kinetics of R6G onto SERS substrates were studied to determine adsorption times and final plateau intensities. Plateau intensities were reached at different times depending on solution concentration. This was expected as the rate of this phenomenon is mass transferred controlled, meaning that higher rates of adsorption for the same molecule should be expected at higher bulk concentrations. As can be seen, the plateau value takes longer to be reached at lower bulk concentrations. Although plateau concentrations are reached within about 2,000 s for the most concentrated solutions, adsorption still appears to take place at the lowest concentration. In addition to allowing us to measure

the actual kinetics of the adsorption process, these measurements also give us an indication of the wait times that need to be observed in in situ measurements for obtaining an accurate reading that corresponds to the equilibrium value. If measurements are taken too fast, this will result in false concentration readings. Our observed time scales agree with other researchers (Tripathi et al., 2015) who performed similar adsorption measurements on a different type of SERS-active substrates for numerous chemical compounds. These researchers also showed that adsorption isotherms thus constructed can yield the equilibrium constants of adsorption and binding energies of the molecules.

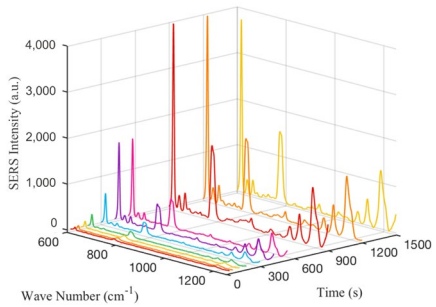

Figure 4: Example of SERS spectra intensity change during R6G adsorption (Concentration: 5x10^{-6} M).

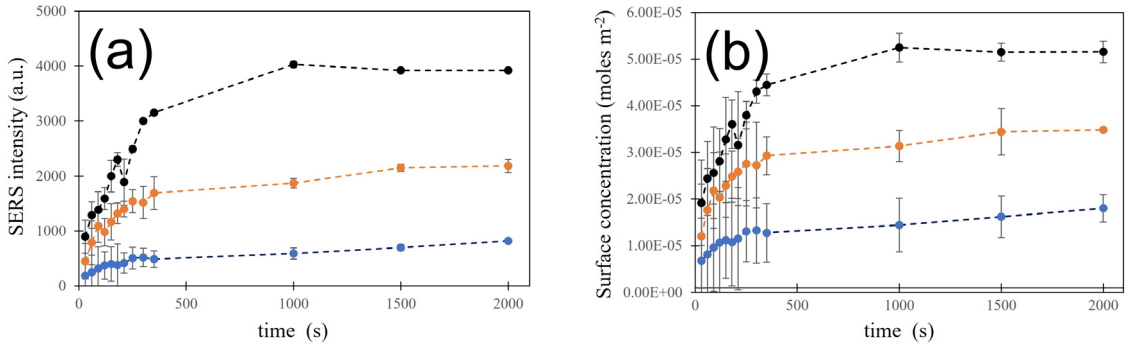

Figure 5: Adsorption kinetics of R6G on the silver SERS-active substrate. (a) SERS signal intensity; (b) Corresponding surface concentration of adsorbed R6G. Conc.: 5x10^{-7} M (●), 1x10^{-6} M (●), 5x10^{-6} M (●).

The corresponding concentrations of R6G adsorbed onto SERS substrate as a function of time can be calculated from the experimental data depicted in Figures 3b and 5a. The kinetics of R6G adsorbed onto AgNPs substrates in Figure 5d illustrates the adsorption rate upon contact of SERS substrates with sample solutions. Knowledge of this phenomenon over time allows for a wider range of application for this SERS detection method. Adsorption concentration as a function of time, Figure 5b, paired with SERS intensity correlated to adsorption concentration, Figure 2a, shows a potential method for immediate analyte concentration detection in sample solutions. In theory, the detection of target molecules can be determined immediately through adsorption kinetics. However, Figure 5b demonstrates that quantification of the detection becomes more accurate as adsorption reaches equilibrium, where error bars between the three concentrations show greater separation.

4. Conclusions

A microfluidic device prototype was developed to introduce sample to a SERS substrate in a controlled manner. An adsorption isotherm was generated for R6G adsorption onto AgNPs by using fluorescence spectroscopy. The amount of R6G adsorbed onto a known surface area of AgNPs at equilibrium was determined and an adsorption isotherm was generated by estimating bulk R6G concentration at equilibrium through deduction. For the range of concentrations used, the adsorption isotherm was given a linear fit. However, more data must be gathered to confirm whether: (1) The fit is linear and represents the linear region of a Langmuir isotherm; (2) The fit is not linear, and a full Langmuir isotherm is seen within this region of concentrations. The adsorption kinetics of R6G onto AgNPs was studied using Raman intensities over time. Using a series of analytical steps, SERS intensity was found to have a linear correlation to adsorbed R6G concentration on the surface of SERS

substrates for the range of concentrations tested (5*10-8 to 5*10-6). Proof of concept was demonstrated for a new method that can be used to rapidly determine the adsorbed concentration of R6G on the surface of AgNPs SERS substrates and concentration of R6G in a sample within the order of magnitude.

Acknowledgements

The authors would like to thank Drs. Joshua Raveendran and Hannah Bacon for their technical assistance and Canada Foundation for Innovation for the support though the John R. Evans Leaders Fund.

References

Andreou C., Hoonejani M.R., Barmi M.R., Moskovits M., Meinhart C.D., 2013, Rapid Detection of Drugs of Abuse in Saliva Using Surface Enhanced Raman Spectroscopy and Microfluidics, ACS Nano, 7:8, 7157-7164. doi:10.1021/nn402563f.

Bacon, H., Docoslis, A., Escobedo C., 2022, Reconfigurable surface enhanced Raman spectroscopy device and method therefor, US Patent 11,237,112.

Dies H., Raveendran J., Escobedo C., Docoslis A., 2017, In situ assembly of active surface-enhanced Raman scattering substrates via electric field-guided growth of dendritic nanoparticle structures, Nanoscale, 9:23, 7847-7857. doi:10.1039/c7nr01743j.

Dies H., Siampani M., Escobedo C., Docoslis A., 2018, Direct detection of toxic contaminants in minimally processed food products using dendritic surface-enhanced Raman scattering substrates, Sensors, 18:8, 2726. doi.org/10.3390/s18082726.

Juncker D., Schmid H., Drechsler, U., Wolf, H., Wolf, M., Michel, B., de Rooij, N., Delamarche, E., 2002, Autonomous Microfluidic Capillary System, Analytical Chemistry, 74, 24, 6139-6144. doi:10.1021/ac0261449

Kong X., Chong X., Squire K., Wang A.X., 2018, Microfluidic diatomite analytical devices for illicit drug sensing with ppb-Level sensitivity, Sensors and Actuators B: Chemical, 15:259, 587-595. doi.org/10.1016/j.snb.2017.12.038.

Maria M.S., Rakesh P.E., Chandra T.S., Sen A.K., 2017, Capillary flow- driven microfluidic device with wettability gradient and sedimentation effects for blood plasma separation, Scientific Reports 7:43457. doi:10.1038/srep43457.

Raveendran J., Docoslis, A., 2021, Detection and quantification of toxicants in food and water using Ag–Au core-shell fractal SERS nanostructures and multivariate analysis, Talanta, 231, 122383. doi.org/10.1016/j.talanta.2021.122383

Shur V. Ya. Et al., 2015, Coffee Ring Effect During Drying of Colloid Drop: Experiment and Computer Simulation, Ferroelectrics, 476, 47-53. doi:10.1080/00150193.2015.998156.

Tripathi A., Emmons E.D., Fountain A.W., Guicheteau J.A., Moskovits M., Christesen S.D., 2015, Critical Role of Adsorption Equilibria on the Determination of Surface- Enhanced Raman Enhancement, ACS Nano, 9:1, 584-593. doi:10.1021/nn5058936.

White I.M., Yazdi S.H., 2013, Multiplexed detection of aquaculture fungicides using a pump-free optofluidic SERS microsystem, Analyst, 138, 100-103. doi:10.1039/c2an36232e

Wilson N.G., Raveendran J., Docoslis, A., 2021, Portable identification of fentanyl analogues in drugs using surface-enhanced Raman scattering, Sensors and Actuators B: Chemical, 330, 129303. doi.org/10.1016/j.snb.2020.129303.